# Measuring Order in Regioregular Poly(3-hexylthiophene) with Solid-State ^{13}C CPMAS NMR

Ryan C. Nieuwendaal,* Chad R. Snyder, and Dean M. DeLongchamp

National Institute of Standards and Technology, 100 Bureau Drive, Gaithersburg, Maryland 20899, United States

Ⓢ *Supporting Information*

ABSTRACT: We report on measurements of order in semicrystalline, high molar mass poly(3-hexylthiophene) (P3HT) by solid-state ^{13}C cross-polarization magic angle spinning (CPMAS) nuclear magnetic resonance (NMR) measurements. The relative degree of crystallinity was estimated for two films with different drying conditions via X-ray diffraction (XRD) and differential scanning calorimetry (DSC). Order determined by ^{13}C NMR does not necessarily correlate with crystallinity, indicating that local order can occur in noncrystalline regions. Slow main chain dynamics influence

the ^{13}C NMR peak widths at lower temperatures (<0 °C), with side chain motions influencing the main chain motions. At higher temperatures (>0 °C), where narrower thiophene resonances are observed, these main chain conformation rearrangements occur on fast time scales (≪3 ms). This room-temperature dynamic disorder suggests that P3HT may be classified as a conformationally disordered (CONDIS) crystal.
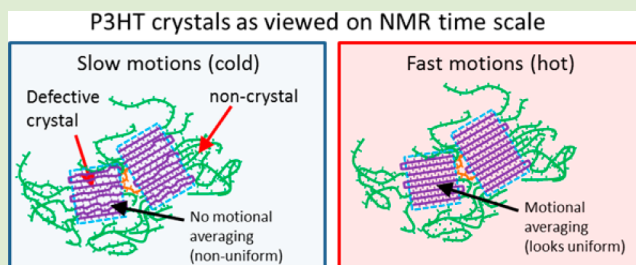
The development of new organic semiconductor materials has recently accelerated, enabling great advancements in the performance of organic thin film transistors (TFTs) and organic photovoltaics (OPVs). Despite these advances, clear relationships between device physics and molecular packing continue to be elusive. The role of order is a particularly persistent question. Although charge transport undoubtedly depends on order,[1−4] the mechanisms of charge transport in semicrystalline semiconducting polymers are generally not well understood. One critical hurdle has been the simple *quantitation* of order, even in the most widely studied semiconducting polymer, poly(3-hexylthiophene) (P3HT). Despite considerable X-ray diffraction (XRD) efforts, only relative estimates of crystallinity have been determined.[5,6] There have been efforts to estimate the absolute fraction of ordered P3HT via linear optical absorption spectroscopy,[7] but the amount of optical aggregate is not proportional to crystallinity.[8,9]

In this article, we introduce solid-state ^{13}C nuclear magnetic resonance (NMR) spectroscopy as an analytical tool for measuring order in semicrystalline, high molar mass P3HT. Unlike XRD, NMR does not quantify long-range order. NMR is instead sensitive to order on subnanometer length scales, probing molecular properties such as distributions of molecular conformations, uniformity of nearest-neighbor molecular packing arrangements, as well as the time scales of motion involved in the disorder.

Although several solid-state NMR studies have been performed on high molar mass, highly regioregular P3HT,[10−14] the ordered fraction was not quantified. A crystallinity quantification study was performed on low molar mass (<10 kDa) P3HT,[15] but as we will show this approach is

not applicable to high molar mass P3HT. Here, we study two different P3HT films having different preparation conditions that result in different amounts of order as determined by XRD and differential scanning calorimetry (DSC). We show that ^{13}C NMR line shape analysis is not as straightforward for P3HT as it is for classic semicrystalline polymers because P3HT chains in noncrystalline regions can exhibit uniform local packing arrangements and molecular conformations. Conversely, as we show from variable-temperature ^{13}C CPMAS NMR, there also exists dynamic main chain disorder within the crystalline regions, which further clouds the distinction between crystalline and noncrystalline regions. These results demonstrate that NMR is a useful tool that can contribute to the emerging, complex understanding of semiconducting polymers as having highly defective crystals[16] and noncrystalline regions with molecular conformation and packing sufficient to support charge transport.[17−19]

XRD patterns were acquired at room temperature for two films with different drying recipes. A "slow-dried" film was drop-cast from chlorobenzene and dried at room temperature over 4−6 h and will be referred to as the "slow-dried" film. A "fast-dried" film was drop-cast from chloroform onto a 70 °C heated Teflon substrate and dried over 3−5 s.

The XRD pattern of the slow-dried film, shown in Figure 1b, exhibits crystalline order with diffraction peaks at 2θ = 5.4°, 10.8°, 16.4°, and 23°; these peaks correspond to the (100), (200), (300), and (020) indices, respectively, of the unit cell for
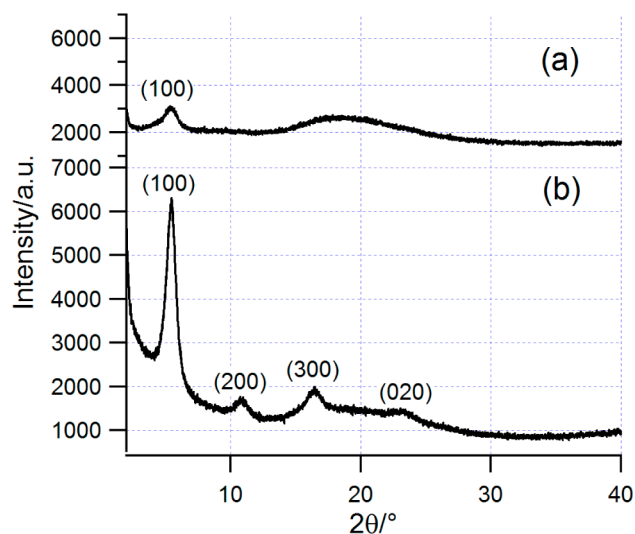
Figure 1. XRD of (a) fast-dried and (b) slow-dried P3HT.

Form 1 P3HT.[20] The broad feature centered at 20° corresponds to disordered chains. As shown in Figure 1a, the intensities of the fast-dried film reflections are significantly lower. The (100) reflection of the fast-dried film is 55% less intense and 50% broader than the slow-dried film, indicating that there is less crystallinity and that the crystals are smaller and/or more defective. However, an absolute crystallinity determination is not possible from these data.

To further assess crystallinity, DSC thermograms were acquired as shown in Figure 2. The slow-dried film exhibits a
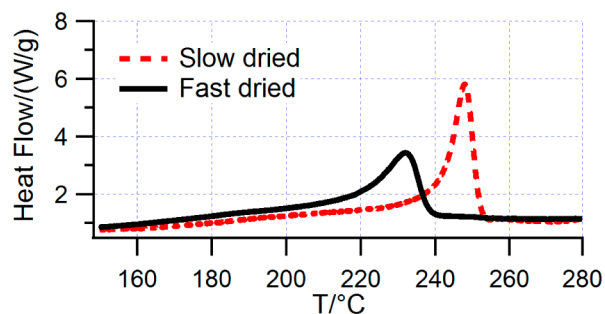

Figure 2. DSC thermograms of the slow-dried and fast-dried films.

melting peak at ≈245 °C (red curve), and the fast-dried film exhibits a broader, lower-temperature melting peak at ≈230 °C (black curve), consistent with the smaller and/or more defective crystals in the fast-dried film as determined by XRD.

The enthalpies of fusion, given in Table 1, were measured from the area under each melting peak. The fast-dried film exhibits a smaller enthalpy (8.9 ± 0.6 J/g) than the slow-dried film (21 ± 2 J/g), indicating ≈58% less crystallinity. This is in close agreement with the XRD (100) reflection, which indicated ≈55% less crystallinity. Despite the similarity, the

Table 1. Ordered Fractions of P3HT Films of Different Drying Rates

film	enthalpy of fusion (J/g)	narrow peak fraction	136 ppm fwhm (Hz)
fast	8.9 ± 0.6	0.47 ± 0.04	50 ± 3
slow	21 ± 2	0.55 ± 0.04	23 ± 3

comparison raises questions regarding how certain types of disorder could impact the underlying physical principles of XRD and DSC crystallinity determination. It is not known how oriented noncrystalline chains influence DSC enthalpy, nor is it known how packing imperfections in crystalline domains or chains on crystal surfaces influence the intensities of XRD reflections or DSC enthalpies.

^{13}C NMR is a classic tool for estimating the degree of order in semicrystalline polymers.[21,22] The ^{13}C resonance positions are sensitive to molecular conformation and nearest-neighbor arrangement, so the resonance peak widths are often used as a diagnostic of order. They can be broadened by either static disorder (nonuniform local packing) or dynamic molecular motions (T_2-type broadening) occurring at frequencies similar to the ^{1}H decoupling field (≈80 kHz). Disorder is considered "static" for motions that occur slower than the inverse of the peak's full-width at half-maximum, fwhm ($1/\pi \cdot$fwhm ≈ 3 ms). A CPMAS spectrum of P3HT taken at 2.35 T is given in Figure 3a, which displays the assignments of ten carbons. Carbons labeled 1−6 (C1−C6) belong to the aliphatic side chain; 7−10 belong to thiophene (C7−C10). The intensities of the spectra in this study are >96% quantitative (see Experimental Section).

There exists a broad underlying feature in the thiophene spectral region (125−135 ppm), which we attribute to disordered main chains. Since the narrow resonances must represent an ordered polymer, we performed $T_{1\rho}{}^H$-filtered CPMAS experiments to separate the spectrum into ordered and disordered P3HT. A CPMAS spectrum with no $T_{1\rho}{}^H$ relaxation filter (Figure 3a) has black lines to represent the intensity values for the disordered (138 ppm) and ordered fractions (136 ppm). A $T_{1\rho}{}^H$-filtered CPMAS spectrum (Figure 3b) includes red lines to mark the 50% intensity values relative to Figure 3a. As shown from Figure 3b, the narrow resonance intensity is approximately 50% of its initial intensity, whereas the broader resonance (138 ppm) is considerably lower, being reduced to 35%, which we represent by a blue line. In Figure 3c we include the difference, [(Figure 3b) − 0.35(Figure 3a)], which exhibits no appreciable intensity at 138 ppm, allowing us to attribute this spectrum to ordered P3HT. Using this spectral editing procedure, we isolated the ordered and disordered components for both films (Figure 3e,f,h,i). Their relative integrated fractions are given in Table 1.

Two important observations can be gleaned from these results. First, the ordered fraction of P3HT is similar for the fast-dried (0.47 ± 0.03) and the slow-dried films (0.55 ± 0.03), despite the significantly different crystallinities observed from the XRD and DSC. Second, the peaks of the slow-dried film's ordered fraction (Figure 3e) are narrower than its fast-dried counterpart (3b), suggesting differences in either the local packing uniformity or dynamic behavior, even within the ordered regions. For example, the fwhm of the 136 ppm resonance is 50 ± 3 Hz (2.0 ± 0.1 ppm) at 2.35 T in the fast-dried film (Table 1, fourth column), whereas the equivalent resonance of the slow-dried film is appreciably narrower, 23 ± 3 Hz or 0.9 ± 0.06 ppm. We chose 136 and 138 ppm as representative frequency positions for analysis because these resonances are due to C7, which is nonprotonated; non-protonated carbons have less dynamic (T_2-type) broadening than protonated carbons and are therefore more sensitive to broadening due to nonuniform local packing. Furthermore, C7 is the most spectrally isolated of the three nonprotonated carbons, allowing for straightforward discrimination of ordered (136 ppm) and disordered fractions (138 ppm).
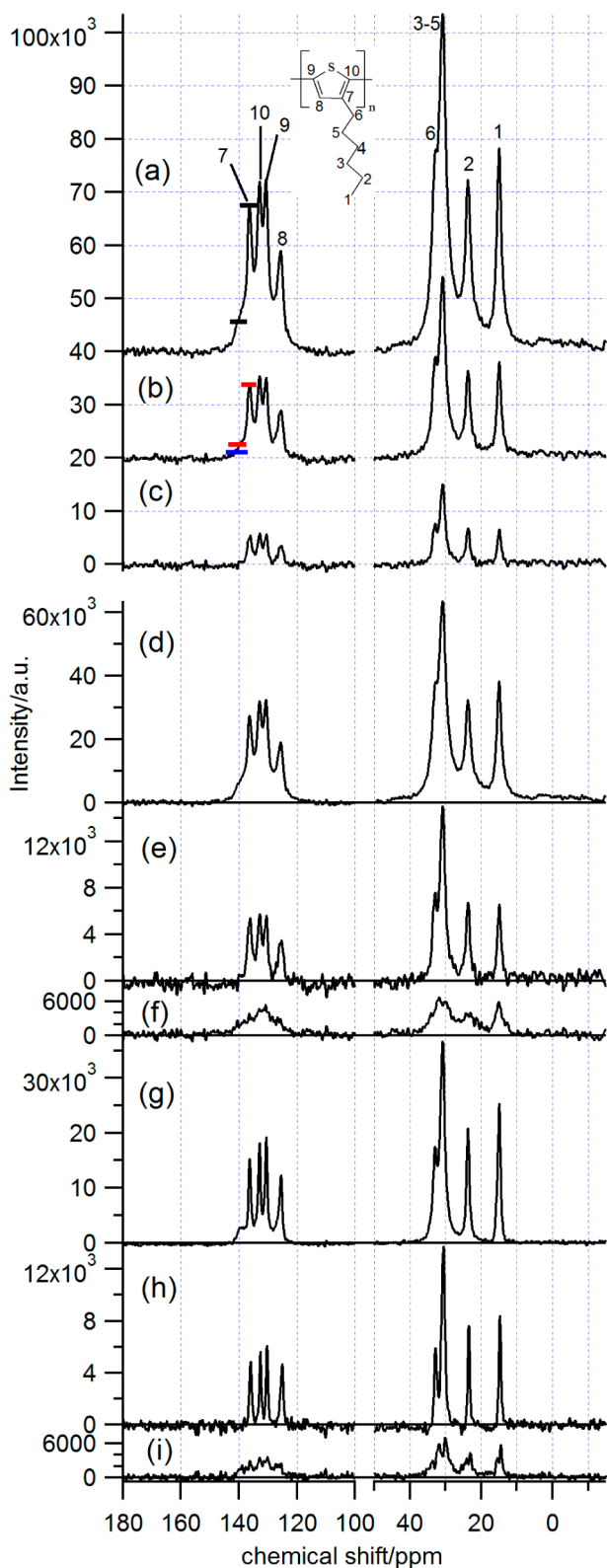
Figure 3. CPMAS spectra of fast-dried P3HT without (a) and with (b) a $T_{1\rho}^{H}$ spectral editing (spin-lock) pulse prior to cross-polarization, as well as the difference spectrum: (c) = (b) − 0.35*(a). CPMAS spectrum for fast-dried P3HT (d) and its ordered (e) and disordered fractions (f). CPMAS spectrum for slow dried P3HT (g) and its ordered (h) and disordered (i) fractions. Spectra were acquired at 2.35 T.

The ^{13}C NMR thiophene peak widths are therefore sensitive to the quality of order within the ordered fraction, whereas the relative intensities of the ordered and disordered contributions describe a bimodal distribution between the two fractions, providing a metric for quantifying order. Because NMR finds so much more order in the fast-dried film than does DSC or XRD, it appears that our approach includes some polymer that is not crystalline in the ordered fraction. A similar discrepancy has been observed in P3HT when comparing optical aggregate presence to the XRD-determined crystallinity.[8,9] With NMR, it is certainly possible that rigid amorphous chains or tie chains between lamella are counted as part of the ordered fraction. Any main chain having a local packing environment or molecular conformation similar to those of crystalline chains would be identified as ordered.

With respect to the quality of order, the narrow resonances of the slow-dried film are expected because the greater crystallinity would, by definition, provide more uniform local packing. It is also possible that chain dynamics within crystals would be restricted and therefore more uniform. There are several potential explanations for the broadening of the fast-dried film's resonances. Oriented noncrystalline chains or crystalline chains close to the fold surface could exhibit (subtly) different chemical shifts if they have different molecular conformations or nearest-neighbor packing. It is also possible that different extents of defects within crystals are responsible for some of the difference.[16] The exact description of disordered subpopulations is not feasible at this point. Breaking down the NMR-determined ordered fraction into finer divisions of order will be the focus of future studies.

The impact of molecular dynamics on disorder was assessed with ^{13}C CPMAS NMR experiments performed at 7.05 T as a function of temperature (Figure 4).[23] All resonances in each spectrum are broad at lower temperatures (<−50 °C) and become narrower upon heating.[24] To probe the nature of this low-temperature broadening, the ^{13}C T_2 (denoted T_{2C}) was measured for a few sample temperatures (as well as magnetic field, 2.35 and 7.05 T) via ^{13}C Hahn echoes (data not shown). The relaxation results show little to no change in T_{2C} with temperature, suggesting that the broadening upon cooling is due to a broader distribution of molecular conformational states being observed on the fixed NMR time scale (≈3 ms, see above), not a change in T_{2C} brought upon by increased mid-kilohertz spectral density and reduced $^{1}H-^{13}C$ decoupling efficiency.

Inspection of the side chain ^{13}C resonances reveals details about their dynamic behavior. Upon heating both films from −80 to 0 °C, a monotonic upfield shift of the ε-methylene ^{13}C chemical shift (C2, ≈23 ppm) occurs due to the γ-gauche effect.[25−27] At higher temperatures, the higher-energy gauche conformations of the hexyl chain become more populated relative to the all-anti configuration, so that the time-averaged shifts move upfield on the ≈3 ms time scale. For example, the C2 resonance (≈23 ppm) shifts upfield with temperature because more C2 carbons are gauche to C5 (and less anti) on the ≈3 ms time scale. No change is observed in either film at temperatures >0 °C, so the time-average fraction of gauche conformations does not appreciably change at these temperatures.

A similar dynamic behavior is observed for the methylene units closer to the main chain as well (carbons C3 through C6). We calculated the total methylene center-of-mass (COM) positions (18−59 ppm range), which are given in Figure 4 by
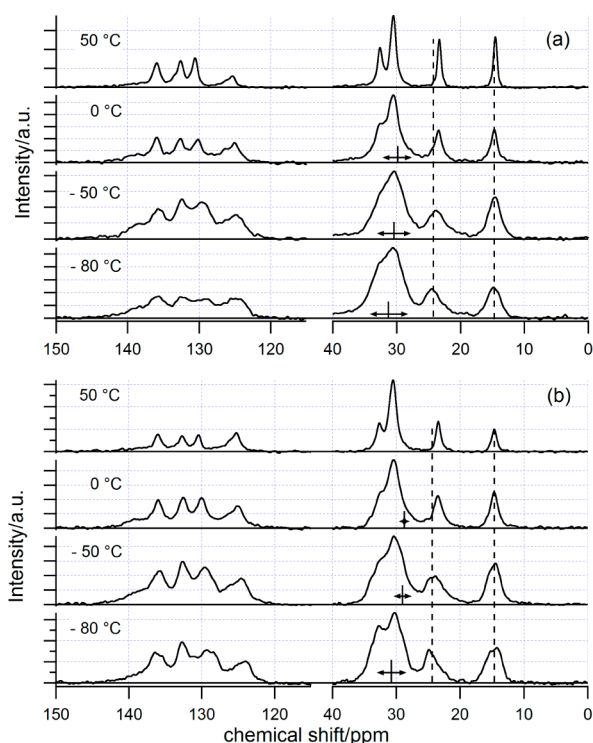
Figure 4. ^{13}C CPMAS NMR spectra of fast-dried (a) and slow-dried (b) P3HT for various temperatures. Vertical dotted lines are given to denote shifts of carbons C2 and C1. Vertical solid lines are given to denote the total methylene COM (C2–C6). Horizontal lines with arrows are given to denote the square root of the second moment of the total methylene signal. Spectra were acquired at 7.05 T.

the vertical solid lines at approximately 30 ppm. The COMs shift upfield with temperature for both films. The peak widths were determined from the square root of the second moment over this same spectral region, indicated by the horizontal lines with arrows at ≈30 ppm in Figure 4. The peaks narrow for both films with increased temperature, indicating that the side chain conformations are more uniform at higher temperatures. The fast-dried film methylene resonances are all broader than the slow-dried ones regardless of temperature, which we ascribe to a broader distribution of side chain conformations.

Surprisingly, the CPMAS spectra indicate that at lower temperatures higher populations of anticonformation side chains can exist in less crystalline films. The fast-dried film (Figure 4a) exhibits more downfield COMs than does the slow-dried film. This indication is further supported by broader ^{1}H NMR resonances in the fast-dried film at these same lower temperatures (data not shown). This result is consistent with packing calculations for crystalline (Form 1) P3HT, which show that the frequency of side chain attachment to the main chain is not sufficiently low to permit side chain interdigitation between vertically adjacent layers, and it is not sufficiently high to permit close side chain packing in a noninterdigitated layer.[28] Hence, the side chains in crystalline (Form 1) P3HT are typically disordered.[29] Thus, there should be no straightforward connection between the side chain conformation (e.g., anti vs gauche) and main chain order. In our NMR results, two films of dramatically different crystallinities have similar side chain conformation and dynamic behavior.

Our results vary from a previous report[14] on primarily Form 2 P3HT which asserted that average side chain conformation could be used as a proxy for crystallinity. In the high molar

mass (Form 1) P3HT films studied here, the side chains in the ordered regions do not exhibit notably different behavior than those in the disordered regions. Side chain packing is inefficient throughout both films, as already established by other methods.[27,29] Since the motions of the highly dynamic side chain groups are complicated by subtleties in main chain packing as well as nearest-neighbor side chain packing,[29] they do not serve well as a general measurement tool for the crystallinity of high molar mass P3HT.

The temperature-dependent ^{13}C CPMAS NMR results also reveal dynamic behavior of the main chain. It is not immediately obvious why the four thiophene resonances would have temperature-dependent broadening similar to the methylene resonances. Although the hexyl chain of P3HT has "liquid-like" behavior,[30] the main chain certainly does not. Furthermore, the γ-gauche effect is a short-range effect (≤4 carbons, 3 bonds), so one would not expect a priori that the main chain chemical shifts would be sensitive to changes in the side chain conformation.[31] The broadening of the main chain resonances upon cooling must therefore be due to a separate conformation change that occurs in concert with the side chain conformation changes. Changes in the side chain and main chain motions and packing are likely to be highly interdependent. The free volume that is available to a side chain, which would influence its likely conformations, is highly dictated by nearest-neighbor side chains as well as main chain packing. Variations in main chain packing within the crystal could occur in multiple forms (e.g., nonuniformity in any of the main chain unit cell angles and spacings), all of which would be highly dependent on the side chain conformation and/or the kinetics of its motion (i.e., amplitudes, time scales).

In this context, and turning again to the room-temperature ^{13}C NMR spectra, the implication of having narrow thiophene resonances in the presence of disordered but highly dynamic side groups is that the side groups must impart some freedom to the main chain such that variations in its local packing and conformation are averaged away on the ≈3 ms time scale. At colder temperatures, with main chain motions being slower than 3 ms, a wider distribution of conformations is sampled, and the ^{13}C NMR spectrum exhibits broader resonances as a result. At room temperature, this variation in main chain conformations likely still exists, but the rapid exchange between states (≪3 ms) renders the system uniform on the ≈3 ms time scale.

The rapid variation in main chain conformation at room temperature suggests that P3HT is a conformationally disordered crystal.[32] Whether these fast molecular rearrangements have implications in the charge transport physics remains to be seen, but one could imagine them playing an important role if the charge hopping rates are on the ≈1 ms time scale.[33] The importance of static vs dynamic main chain disorder has only recently been addressed by computational studies.[34] Our results suggest NMR could have a role in contributing to these modeling efforts.

In conclusion, our results show that ^{13}C CPMAS NMR can be used to measure local order in semiconducting, semicrystalline polymers such as P3HT. This local order, which is defined in terms of the uniformity of molecular conformation and local packing arrangement, does not necessarily correlate to crystallinity. It nevertheless offers a powerful alternative structure measurement tool, which shows that local order exists in noncrystalline regions. A coupling between the dynamic behavior of the side chains and the main chains is

shown by temperature-dependent measurements, with apparent main chain uniformity at room temperature revealed to be the product of time-averaged rapid conformation variation. The presence of this disorder within the crystal suggests that P3HT may be a conformationally disordered (CONDIS) crystal.

EXPERIMENTAL SECTION

Materials. P3HT (Plexcore 2100, Plextronics Inc., Pittsburgh, PA) was used as received. According to the manufacturer the P3HT is ultrahigh purity (<25 ppm trace metals) and highly regioregular (>98% head-to-tail), with a number averaged molar mass of 64 500 g/mol and polydispersity index (PDI) of ≤2.5. The slow-dried film was prepared by drop casting a 15 mg/mL solution of P3HT in chlorobenzene into a Teflon well plate; films formed in approximately 4−6 h. The fast-dried film was prepared by drop casting a 15 mg/mL solution of P3HT in chloroform (>99.8%) onto a 70 °C heated Teflon substrate; films formed in <5 s. The chloroform (>99.8%) and chlorobenzene (>99.8%) were used as received. Films were sliced into approximately 50 fine flakes of ≈0.1 mm dimension and (lightly) pressed into disks to ensure isotropy and homogeneity in the NMR and XRD experiments.

DSC. DSC was performed on a PerkinElmer DSC8500 HyperDSC equipped with a CLN2 liquid nitrogen cooler and a helium purge.[35−37] All measurements were performed on samples with masses between 0.3 and 0.6 mg in foil packets with masses of ≈1.9 mg at heating rates of 100 °C/min. Calibration of heat flow (and temperature) was achieved using an indium sample NIST Standard Reference Material 2232 at the same heating rate with a mass of ≈0.5 mg. Additional temperature calibration was performed with a lead standard of similar size. The temperature calibration was validated by placing a ≈0.2 mg sample of indium on a ≈0.3 mg sample of P3HT, and the indium melting onset was with ≈0.1 °C of the calibrated value. HyperDSC was used to minimize both the required sample mass (to enable replicate studies) and any melting−recrystallization processes that might occur on heating. Enthalpies of fusion were estimated based on averages of 3 to 4 samples, and the standard deviations provided are the best estimate of one standard deviation in the experimental uncertainty.

XRD. Measurements were performed on a Rigaku SmartLab X-ray diffractometer equipped with a D/teX Ultra high-speed one-dimensional X-ray detector. Measurements were performed with Cu Kα radiation with a wavelength of 0.154 nm, from 2θ = 2 to 40° in steps of 0.01° at 3 s per step.

NMR. Experiments that were performed at 300 MHz (7.05 T) were on a Bruker DMX300 spectrometer utilizing a 4 mm triple resonance magic angle spinning probe. Each sample (≈30 mg) was pressed into a 4 mm × 4 mm disk and placed into a 4 mm ZnO_2 rotor and spun at 9800 (or 4900) ± 1 Hz. CPMAS was performed under the following conditions: 75.46 MHz ^{13}C frequency, 300.13 MHz ^{1}H frequency, 3.2 μs $\pi/2$ ^{1}H excitation pulse, 2−3 ms contact time, 52 kHz ^{13}C contact pulse, 62 (or 57 kHz) ^{1}H contact pulse, 78 kHz TPPM ^{1}H decoupling, 1024 data points with 64 512 zero filling points, 4096 scans, 20 μs dwell time, 5 s recycle delay. The ^{1}H TPPM decoupling[38] had the following parameters: 2 ppm ^{1}H frequency (from tetramethylsilane, TMS), 170° flip angle, 15° modulation angle. The Hartmann−Hahn match was optimzied on crystalline powders of adamantane, which was also served for calibration of the ^{13}C frequency scale (adamantane CH_2 set to 38.48 ppm).[39]

The variable-temperature experiments were performed using a liquid nitrogen heat exchanger with nitrogen drive gas. Temperatures were calibrated with ^{207}Pb magic angle spinning NMR spectra on an internal standard of lead nitrate.[40]

Experiments that were performed at 100 MHz (2.35 T) were on a Tecmag Apollo spectrometer, ultrawide bore Nalorac magnet, and home-built 7.5 mm double resonance magic angle spinning probe. Each sample (≈100 mg) was pressed into a 6 mm × 7 mm disk, placed into a Macor rotor, and spun at 3800 ± 100 Hz. CPMAS was performed with the following conditions: 25.19 MHz ^{13}C frequency, 100.16 MHz ^{1}H frequency, 3.2 μs ^{1}H $\pi/2$ pulse, 2 ms contact time, 72

kHz ^{13}C contact pulse, 68 kHz ^{1}H contact pulse, 78 kHz continuous wave (cw) decoupling, 100 μs dwell time, 600 data points with 15 784 zero filling points, 2048−8196 scans, and 4 s recycle delay. The ^{1}H cw decoupling frequency was set to 2 ppm (relative to TMS at 0 ppm). The close agreement between a CPMAS spectrum taken at 2.35 T under these cross-polarization conditions and a spectrum taken under single pulse excitation conditions (>99% quantitative) enabled us to quote the level of quantitation in this study. The level of quantitation (96%) was estimated by computing the intensity of the difference spectrum (<4%), i.e., CPMAS-SPE. SPE experiments were acquired using a 75 s recycle delay. The T_1^{C}'s of this P3HT sample are given in the Supporting Information. CPMAS spectra were also acquired as a function of contact time, match conditions, magic angle spinning rate, and temperature. These background experiments lend confidence to our quantitation under these experimental conditions. The CPMAS spectra taken at 7.05 T at higher temperatures (> 25 °C) and higher magic angle spinning rates (> 5 kHz) were somewhat less quantitative.

ASSOCIATED CONTENT

⑤ Supporting Information

The T_1^{C}'s of P3HT used for quantitation. This material is available free of charge via the Internet at http://pubs.acs.org.

AUTHOR INFORMATION

Corresponding Author

*E-mail ryan.nieuwendaal@nist.gov.

Author Contributions

The manuscript was written through contributions of all authors. All authors have given approval to the final version of the manuscript.

Notes

The authors declare no competing financial interest.

ACKNOWLEDGMENTS

REFERENCES

(1) Sirringhaus, H.; Brown, P. J.; Friend, R. H.; Nielsen, M. M.; Bechgaard, K.; Langeveld-Voss, B. M. W.; Spiering, A. J. H.; Janssen, R. A. J.; Meijer, E. W.; Herwig, P.; de Leeuw, D. M. *Nature* **1999**, *401*, 685−688.

(2) Street, R. A.; Northrup, J. E.; Salleo, A. *Phys. Rev. B* **2005**, *71*, 165202.

(3) Jimison, L. H.; Toney, M. F.; McCulloch, I.; Heeney, M.; Salleo, A. *Adv. Mater.* **2009**, *21*, 1568−1572.

(4) Kline, R. J.; Mcgehee, M. D.; Toney, M. F. *Nat. Mater.* **2006**, *5*, 222−228.

(5) Baker, J. L.; Jimison, L. H.; Mannsfeld, S.; Volkman, S.; Yin, S.; Subramanian, V.; Salleo, A.; Alivisatos, A. P.; Toney, M. F. *Langmuir* **2010**, *26*, 9146−9151.

(6) Gomez, E. D.; Barteau, K. P.; Wang, H.; Toney, M. F.; Loo, Y.-L. *Chem. Commun.* **2011**, *47*, 436−438.

(7) Clark, J.; Silva; Friend, R. H.; Spano, F. C. *Phys. Rev. Lett.* **2007**, *98*, 206406.

(8) Jimison, L. H.; Himmelberger, S.; Duong, D. T.; Rivnay, J.; Toney, M. F.; Salleo, A. *J. Polym. Sci., B: Polym. Phys.* **2013**, *51*, 611−620.

(9) Shin, N.; Richter, L. J.; Herzing, A. A.; Kline, R. J.; DeLongchamp, D. M. *Adv. Energy Mater* **2013**, *3*, 938−948.

(10) Yawaza, K.; Inoue, Y.; Yamamoto, T.; Asakawa, N. *Phys. Rev. B* **2006**, *74*, 094204.

(11) Yazawa, K.; Inoue, Y.; Shimizu, T.; Tansho, M.; Asakawa, N. *J. Phys. Chem. B* **2010**, *114*, 1241−1248.

(12) Yang, C.; Hu, J. G.; Heeger, A. J. *J. Am. Chem. Soc.* **2006**, *128*, 12007−12013.

(13) Mens, R.; Demir, F.; Van Assche, G.; Van Mele, B.; Vanderzande, D.; Adriaensens, P. *J. Polym. Sci. A: Polym. Chem.* **2012**, *50*, 1037−1041.

(14) Martini, F.; Borsacchi, S.; Spera, S.; Carbonera, C.; Cominetti, A.; Geppi, M. *J. Phys. Chem. C* **2013**, *117*, 131−139.

(15) Pascui, O. F.; Lohwasser, R.; Sommer, M.; Thelakkat, M.; Thurn-Albrecht, T.; Saalwachter, K. *Macromolecules* **2010**, *43*, 9401−9410.

(16) Rivnay, J.; Noriega, R.; Kline, R. J.; Salleo, A.; Toney, M. F. *Phys. Rev. Lett.* **2011**, *B84*, 045203.

(17) Zhang, X.; Bronstein, H.; Kronemeijer, A. J.; Smith, J.; Kim, Y.; Kline, R. J.; Richter, L. J.; Anthopoulos, T. D.; Sirringhaus, H.; Song, K.; Heeney, M.; Zhang, W.; McCulloch, I.; DeLongchamp, D. M. *Nat. Commun.* **2013**, *4*, 2238.

(18) Street, R. A. *Science* **2013**, *341*, 1072−1073.

(19) Noriega, R.; Rivnay, J.; Vandewal, K.; Koch, F. P. V.; Stingelin, N.; Smith, P.; Toney, M. F.; Salleo, A. *Nat. Mater.* **2013**, *12*, 1037.

(20) Prosa, T. J.; Winokur, M. J.; Moulton, J.; Smith, P.; Heeger, A. J. *Macromolecules* **1992**, *25*, 4364−4372.

(21) Schmidt-Rohr, K.; Spiess, H. W. *Multidimensional NMR and Polymers*; Academic Press Limited: London, 1994.

(22) Bovey, F. A.; Mirau, P. A. *NMR of Polymers*; Academic Press, Inc.: San Diego, 1996.

(23) We note that spectra taken at ambient temperature and lower field (Figure 3) or lower temperatures (<0 °C) and higher field (Figure 4) should be thought of as quantitative to within ±2%. On the other hand, those at 7.05 T and at temperatures >25 °C are somewhat less quantitative. This is clear from the nonquantitative resonance intensities shown at 50 °C (top spectra, Figure 4b,c).

(24) We note that over the temperature range of these experiments magic angle spinning ^{79}Br NMR spectra of KBr show no notable change in line shape or number of spinning sidebands, which indicates that peak width changes as a function of temperature seen in Figure 4b,c are not attributable to deviations from the magic angle. Furthermore, there is no appreciable change in ^{1}H decoupling field (B_1^H > 70 kHz) at these lower temperatures.

(25) Grant, D. M.; Paul, E. G. *J. Am. Chem. Soc.* **1964**, *86*, 2984−2990.

(26) Tonelli, A. E. *Macromolecules* **1978**, *11*, 565−567.

(27) Earl, W. L.; VanderHart, D. L. *Macromolecules* **1978**, *12*, 762−767.

(28) Kline, R. J.; DeLongchamp, D. M.; Fischer, D. A.; Lin, E. K.; Richter, L. J.; Chabinyc, M. L.; Toney, M. F.; Heeney, M.; McCulloch, I. *Macromolecules* **2007**, *40*, 7960.

(29) Orbzut, J.; Page, K. A. *Phys. Rev. B* **2009**, *80*, 195211.

(30) Gurau, M. C.; Delongchamp, D. M.; Vogel, B. M.; Lin, E. K.; Fischer, D. A.; Sambasivan, S.; Richter, L. J. *Langmuir* **2007**, *23*, 834−842.

(31) Whitesell, J. K.; Minton, M. A. Stereochemical Considerations. *Stereochemical Analysis of Alicyclic Compounds by C-13 NMR Spectroscopy*, 1st ed.; Chapman and Hall Otd: London, 1987; pp 37−40.

(32) Wunderlich, B.; Möller, M.; Grebowicz, J.; Baur, H. *Adv. Polym. Sci.* **1988**, *87*, 1−121.

(33) Shuttle, C. G.; O'Regan, B.; Ballantyne, A. M.; Nelson, J.; Bradley, D. D. C.; de Mello, J.; Durrant, J. R. *Appl. Phys. Lett.* **2008**, *92*, 093311.

(34) McMahon, D. P.; Troisi, A. *ChemPhysChem* **2010**, *11*, 2067−2074.

(35) Pijpers, T. J. F.; Mathot, V. B. F.; Goderis, B.; Scherrenberg, R. L.; van der Vegte, E. *Macromolecules* **1999**, *32*, 3601−3613.

(36) Poel, G. V.; Mathot, V. B. F. *Thermochim. Acta* **2006**, *446*, 41−54.

(37) Cheruthazhekatt, S.; Pijpers, T. F. J.; Harding, G. W.; Mathot, V. B. F.; Pasch, H. *Macromolecules* **2012**, *45*, 2025−2034.

(38) Bennett, A. E.; Rienstra, C. M.; Auger, M.; Lakshmi, K. V.; Griffin, R. G. *J. Chem. Phys.* **1995**, *103*, 6951.

(39) Morcombe, C. R.; Zilm, K. W. *J. Magn. Reson.* **2003**, *162*, 479.

(40) Bielecki, A.; Burum, D. *J. Magn. Reson. A* **1995**, *116*, 215−220.